GUTHRIE, R.I.L., ISAC, M., and LIN, Z. A fluid dynamics simulation of chromium recovery from AOD slags during reduction with ferrosilicon additions. *VII International Conference on Molten Slags Fluxes and Salts,* The South African Institute of Mining and Metallurgy, 2004.

A fluid dynamics simulation of chromium recovery from AOD slags during reduction with ferrosilicon additions

R.I.L. GUTHRIE*, M. ISAC*, and Z. LIN†
*McGill Metals Processing Centre, McGill University, Montreal, Canada
†Danielli, Beijing,China

The kinetic and thermodynamic efficiencies of chromium recovery from the slag in an AOD process during the slag de-oxidation period with ferrosilicon is a complex process affected by slag basicity, temperature, the dissolution kinetics of the reducing agents, and intermixing of the slag/metal/alloy addition phases within the vessel. The present work focused on a study and simulation of the fluid dynamics and mixing behaviour of ferrosilicon additions in the AOD process for the production of stainless steel. In order to visualize the mixing behaviour, a two dimensional slice model of an AOD vessel was first built and filled with $ZnCl_2$ solution and then covered with silicone oil in order to represent the bulk liquid steel and slag phases, respectively. The injection of argon/oxygen process gases was simulated using air or helium. Particle trajectories and intermixing of the phases was monitored with a high-speed camera. To simulate the 75FeSi additions, glass spheres were used. A three-dimensional version of the AOD model was then constructed in order to confirm the adequacy of the slice model. Similar particle mixing behaviour was observed. Both models demonstrated that the ascending gas/liquid plume created two asymmetric mixing zones: a smaller rapidly re-circulating mixing zone adjacent to the side-wall locating the tuyere(s), and a larger mixing zone in the main part of the vessel. The process efficiency during the reduction period is governed by the thermal behaviour of ferroalloy as well as the mixing efficiency in the main large mixing zone. To enhance the recovery efficiency for chromium, small Fe-Si particles are suggested, given their wide distribution within the slag phase, and their large interfacial areas and rapid melting times for Cr_2O_3 reduction from the slag.

Keywords; modelling, ferrosilicon, chromium oxidation, AOD steelmaking.

Introduction

The Argon-Oxygen-Decarburization (AOD) process, which was developed by the Linde Corporation in the 1960s, is the most commonly used process for the economic production of high quality stainless steel. In the AOD refining process, charge materials are added to the liquid metal from the top of vessel, while argon-oxygen (or nitrogen) mixtures are injected into the molten metal from an array of typically five shrouded tuyeres, 12.2–15.3 mm. in diameter, installed on the side wall of the converter. The profile and dimensions of a typical 85 ton AOD converter is given in Figure 1.

By diluting oxygen gas with argon or nitrogen, it is possible to charge lower cost high carbon-ferrochrome vs. low carbon Fe-Cr additions, and to then selectively decarburize the stainless steel melts to low levels of dissolved carbon, without excessive oxidation of chromium into the slag phase. Nonetheless, a typical slag composition following the end of the decarburization period for an 18% Cr and 8% Ni steel will contain about 30 to 40 % Cr_2O_3 in the slag phase. For the process to be economical, the valuable elements that have been oxidized need to be recovered. This is normally achieved by adding 75% FeSi ferroalloy lump additions, together with some fluxing agents, to the slag at the end of the decarburization operation. The reduction reaction is completed through vigorous stirring with argon injected through the side

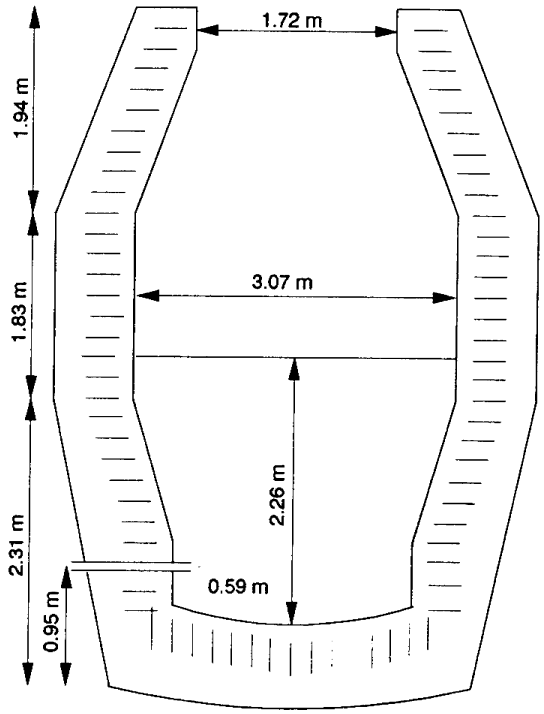

Figure 1. Typical shape and dimensions of a cylindrical AOD vessel

tuyeres for 5 to 17 minutes (0.4 to 1.2 Nm^3/min t for the 85 ton AOD vessel shown in Figure 1). At the end of the reduction reaction, the slag becomes fluid and contains from 0.1% to 5% Cr_2O_3[1]. The overall reaction for the reduction of oxidized chromium in the slag by ferrosilicon alloy additions can be expressed as follows:

$2Cr_2O_3$(in slag) + 3Si (granules/lumps) = $3SiO_2$ (in slag) + 4Cr (steel bath)

The kinetic and thermodynamic efficiencies of chromium recovery in the reduction reaction shown above is evidently complex and is affected by variables such as slag basicity, temperature, dissolution kinetics of the reducing agents, and mixing behaviour within the vessel. However, if all other variables are held constant for a given AOD operation, any difference in the performance of specific forms of ferro-silicon additions may be attributed to different dissolution kinetics. In a collaborative study with Dr Young Lee, of ELKEM, an investigation of the fluid mechanic behaviour of ferrosilicon granules vs. lump ferrosilicon additions to AOD furnaces was made, in order to learn how they were entrained within the vessel, and to determine whether the replacement of lump additions with granules was cost effective. Another objective of this joint study was to determine whether the severity of refractory erosion during the reduction period might be moderated with faster dissolving granules leading to shorter processing times.

From the academic point of view, it was not clear how an upper slag phase (2" to 3" thick) affects the overall fluid dynamics within such a vessel, and the slag's role in the attendant mixing behaviour of ferroalloy additions in AOD operations. Although many theoretical and experimental investigations have been carried out in the past on process dynamics and alloy additions in gas stirred ladles, numerical, as well as most physical models of such systems, have generally ignored the presence of any overlying slags.

Mazumdar *et al.* once carried out a study in order to identify the possible effects of an upper slag phase on the fluid dynamics of gas stirred ladles[2,3]. Following extensive flow velocity measurements using Laser Doppler Velocimetry, they found that the horizontal velocity components near the 'slag/metal' interface were considerably damped through interactions of the floating oil phase with the bulk liquid. By comparing three different modes of energy dissipation: 'slag' droplet creation, 'slag' droplet suspension, and 'slag/metal' interface distortion, they concluded that a significant portion of the input energy to a gas stirred ladle was dissipated in the potential energy requirements associated with distortion of an overlying slag phase during industrial argon/nitrogen stirred ladle operations. This dissipation in input energy would lead to a decrease in both the mean and turbulence kinetic energies of motions within the bulk steel and therefore significantly affect the efficiencies of numerous processing operations, such as the dispersion and dissolution of alloy additions.

Summarizing, there are many grey areas in need of study in order to optimize industrial AOD operations. As a first step towards understanding the kinetic performance of AOD reactors, it was decided that a fluid dynamic investigation of bulk fluid motions was needed.

Experimental method and procedures

One main feature of an AOD vessel is to inject the process gases (O_2, Ar/N_2) through a cluster of 4 to 7 submerged, side-mounted tuyeres of 3/8" to 5/8" I.D. Although a recent modification introduces a top oxygen lance, the configuration of submerged sideways injection of argon/nitrogen-oxygen mixtures remains the principle mode during the slag reduction period, since top oxygen flow is cut to zero during the slag reduction stage for recovery of chrome to the melt.

The AOD operations that were simulated were for an 85 ton vessel whose dimensions are shown in Figure 1 In order to determine the equivalent gas flow rates needed for the modelling experiments on a one-fifth scale 3D model, one has to consider the modelling criteria needed for similitude of fluid flow behaviour. For this, some authors have used equivalent specific energy input (W/kg) as the modelling criteria in their modelling studies of submerged gas-liquid systems[2,4]. By considering the following contributions to energy input into a submerged gas-liquid system: (1) power through expansion of gas at unaltered pressure; (2) power through isothermal expansion of gas plume; and (3) kinetic energy of injected gas, one can show that the total specific energy input is:

$$\varepsilon_m = \frac{\varepsilon_1 + \varepsilon_2 + \varepsilon_3}{m_1} = 371\frac{QT_1}{m_1}\left[\left(1 - \frac{T_o}{T_1}\right) + \ln\frac{P_1}{P_2}\right] + 0.811\frac{Q^3\rho_g^{\,3}}{m_1 n_o^{\,2} d_o^{\,4} \rho_{g.1}^{\,2}}$$

where, Q = gas flow rate at normal pressure and 273K,(Nm^3/s), m_1 = weight of hot liquid metal, (kg), T_1 = temperature of hot metal (K), T_0 = room temperature (K), P_2 = pressure of injected gas at bath surface, (Pa), P_1 = pressure of injected gas at tuyere exit (Pa), ρ_g = density of gas at normal pressure and 273 K (kg/m^3), n_0 = number of tuyeres, d_0 = tuyere diameter (m).

By considering the following typical industrial conditions for the 85 tonne prototype AOD vessel, Q = (0.4 Nm^3/min t to 0.8 Nm^3/min t) × 85 t = 0.567 to 1.134 Nm^3/s, m_1 = 85 × 10^3 kg, T_1 = 1873 K, T_0 = 298 K, P_2 = 101.3 × 10^3 Pa, P_1 = $P_2 + \rho_l g h_l$ = 101.3 × 10^3 + 6800 × 9.8 × 1.67 = 212.6 × 10^3 Pa, ρ_g = 1.784 kg/m^3 (Ar), $\rho_{g.1} = \frac{\rho_1}{\rho_2}\rho_g = \frac{212.6\times10^3}{101.3\times10^3}\times1.784 = 3.744\ kg/m^3$, $n_o = 5$, $d_o = 1.27\times10^{-2} m$, one can deduce that the above conditions represent a range of specific energy input from 8.41 to 23.30 W/kg for the fifth scale model. Unlike a ladle system, where the kinetic energy input is usually less than 5% and is relatively negligible[2], it is noted that the contribution of input kinetic energy of the injected argon gas can represent up to 37% of the total specific energy input in the prototype AOD vessel. This suggests the importance of modelling the inertial forces of the injected gases in influencing the fluid flow in AOD operations at high gas flow rates. This is further explained in the following analysis.

For fluid behaviour in submerged gas-liquid systems, the modified Froude number is usually suggested as the modeling criterion[4]. According to its definition,

$$Fr` = \frac{\rho_{g,l} u^2}{(\rho l - \rho_{g,l}) g L}$$

The modified Froude number represents the ratio of the inertial forces of the injected gas versus the buoyant forces on the injected gas. These are thought to be the two most important forces dominating fluid flow behaviour in submerged gas-liquid systems. For the industrial conditions commonly seen for the 85 tonne AOD vessel, P_2 = 101.3 x 10^3 Pa, $P_1 = P_2 + \rho_l g h_l$ = 101.3 × 10^3 + 6800 × 9.8 × 1.67 = 212.6 × 10^3 Pa, ρ_g=1.784 kg/m^3 (Ar), we have:

$\rho_{g.1} = \frac{\rho_1}{\rho_2}\rho_g = \frac{212.6\times10^3}{101.3\times10^3}\times1.784 = 3.744\ kg/m^3$, ρ_l = 6800 kg/m^3, L = 1.67 m, $n_0 = 5$, $d_o = 1.27\times10^{-2}\ m$, Q =(0.4 Nm^3/min t to 0.8 Nm^3/min t) x 85 t = 0.567 to 1.134 Nm^3/s, giving u ~ 425 to 851 m/s. Such velocities reveal that gas flows issuing from the submerged nozzles are supersonic under industrial conditions. Inserting appropriate values for the parameters in the modified Froude number, values in the prototype AOD vessel should therefore range from 6 to 24, indicating that the inertial and buoyant forces are the same order of magnitude. It should be noted that the emulsification of two liquid phases in aqueous modelling is energetically much easier than in slag/metal systems, primarily due to their smaller differences in density. As a result, the aqueous modelling experiments were started at a low gas flow rate and stopped at a gas flow rate at which the two liquid phases became fully emulsified, regardless of the gas flow rates derived from the equivalent modified Froude number or specific energy input.

Ferroalloy hydrodynamics

To model intermixing behaviour, or trajectories, of alloy additions in liquid steel, the essential parameters and experimentation have to be determined in order to ensure a correspondence between model and prototype systems (5). Since the hydrodynamic simulation of the entrainment and mixing behaviour of alloy additions involves treating the motion of a buoyant lump (a sphere, for simplicity) of relatively constant diameter as it moves through a swirling flow of liquid steel, one can use the differential equation technique to determine what important parameters need to be considered, and therefore how to set about modelling mixing behaviour of alloy additions.

Provided the added mass coefficient is identical for both large and small spheres, the drag coefficient C_D is numerically equivalent (true provided Reynolds number ~10^4 or more), the solid/liquid density ratio is the same, the Froude number is the same for both model and prototype, provided $d_{p2} = \lambda\, d_{p1}$, $\gamma_2 = \gamma_1$, $u_{r2} = \lambda^{1/2}\, u_{r2}$.

In order to visualize intermixing behaviour, a two-dimensional slice model of an AOD vessel was constructed using two one-inch thick vertical panels of crystaplex. This approach allows one to simulate a slice volume of an industrial AOD vessel. Figure 2 shows the geometry and dimensions of the slice model constructed. The separation distance between the two crystaplex panels was 26 mm, in order to accommodate large sized objects simulating 75FeSi lump alloy additions, and eliminate the possibility of their becoming jammed sideways.

For experiments, the slice model vessel was filled with water (ρ = 1000 kg/m^3) to a depth of 0.5 m for simulating the mixing behaviour of 75FeSi alloys in a slag- free steel melt and later with zinc chloride solution (ρ = 1700 kg/m^3) covered by 50 mm thick silicone oil (ρ = 970 kg/m, μ = 340 mPa·s) on top in order to approximate the situation of slag covered steel melt. Wooden particles were added to the water or zinc chloride solutions during these experiments, to simulate the addition of 75FeSi alloy particles during the reduction period in the AOD process. These wooden particles representing 75FeSi alloy were prepared with correct density ratios of the alloy to steel ($\gamma=\rho_{75FeSi}/\rho_{steel}$=2900/6800=0.41) for both water and zinc chloride solutions, and were in the shape of spheres with sizes in the range of 2 mm, 5 mm, 10 mm diameters and of discoids with the dimensions of 25 mm diameters x 8 mm thick.

The submerged side-blown tuyere was modelled by installing a single 4 mm diameter pipe horizontally on the side of the vessel at a height of 150 mm above the inside base and 350 mm below the surface of water or zinc chloride solution. The injection of process gases was simulated by air or helium. In order to examine the effect of vessel position, experiments were also carried out with the vessel in the tilted, as well as upright, modes. Mixing behaviour was monitored with a high-speed video camera.

Three-dimensional model

In preparing the study of mixing behaviour of 75FeSi alloys in a two-dimensional slice model as depicted above, one major concern was that the flow patterns established in the slice model might be such as to severely modify the nature of gas phase-liquid interactions and the attendant behaviour of particles. There was also some concern that the two-dimensional nature of the flow in the slice model prevents recirculation of liquid back towards the penetrating gas jet and therefore produces distorted flow patterns. An approximate one-fifth scale three-dimensional model was therefore constructed, whose dimensions are given in Figure 3, fitted with 5 tuyeres (I.D. 4 mm), whose nozzles pointed towards the central axis of the vessel. The angle subtended between the five equi spaced tuyeres was 20°.

Similar experimental procedures to the two-dimensional model were applied. The vessel was filled with water to a depth of 250 mm for simulating the mixing behaviour of 75FeSi alloys in a slag-free melt, and with zinc chloride solution to a depth of 420 mm (ρ = 1700 kg/m^3) covered by a 50 mm thick silicone oil (ρ = 970 kg/m^3, μ = 340mPa·s) on top, in order to approximate the situation of slag covered steel melts. To simulate the 75%FeSi, some 100 spherical particles were fabricated. These particles were dropped into the bath from a height of 0.7 m above the bath surface. The 0.7 m free fall gave an entry velocity of 3.7 m/s to ensure Froude similitude for corresponding entry velocities between the model and the 85 ton prototype vessel. In the prototype vessel, ferroalloy particles are normally charged

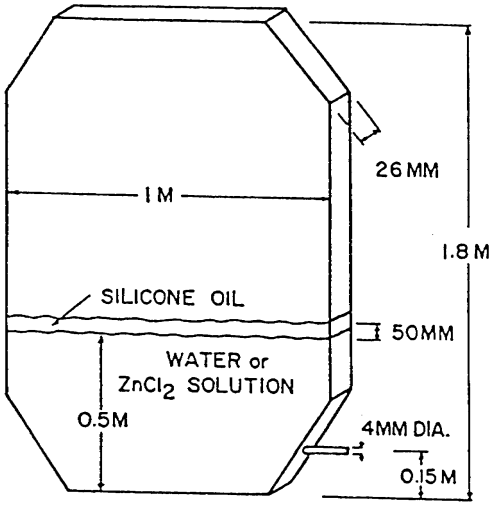

Figure 2. Physical dimensions of the two-dimensional slice model of a generic AOD processing vessel

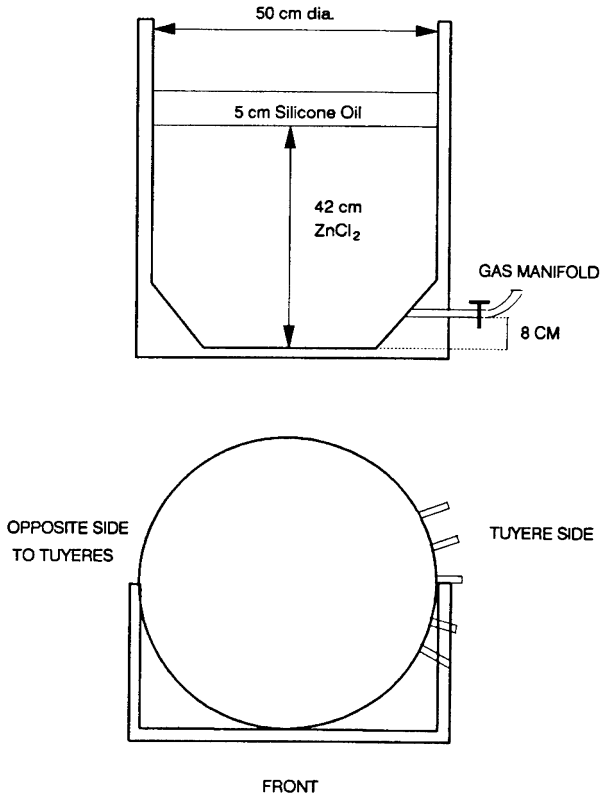

Figure 3. Physical dimensions of a generic 3D AOD stainless steelmaking vessel

from the mouth of the vessel (3.5 m high above the bath surface) and have an entry velocity of 8.3 m/s. It should be noted that only air was used to simulate process gases in the three-dimensional model experiments.

Experimental results

Two-dimensional slice model

Slag free steel model

Having filled to a height of 0.5 m with water, the wooden particles simulating 75FeSi alloy lump and granule additions were made. Air was blown into the vessel at various flow rates in the range of 20 to 120 SLPM, during these alloy additions. Owing to the general turbulence and splashing generated by the submerged gas jet, very fine air bubbles became entrained in the recirculating liquid, and these provided an excellent means for flow visualization. Figure 4 provides a schematic visualization of fluid flow and the mixing behaviour of particles simulating 75FeSi alloy when air was injected to the water-filled slice model.

The forward penetration of the side blown air jet into the reaction vessel was not great. Although an increased air flow rate tended to increase the forward penetration somewhat, the overall horizontal forward penetration was limited to the range of 50 to 150 mm from the top to the tuyere. As soon as the gas exited the tuyere, the gas/liquid plume rose quickly. However, the rising plume was bent back towards the adjacent side wall of the vessel due to liquid recirculating back to the plume from the bulk of the vessel. The deflected gas/liquid plume rose quickly in a pulsating mode up the side wall. This generates another rapidly recirculating flow in the narrow region between the rising plume and side wall. At the gas/melt interface, the majority of air separated from the gas/liquid plume. However, some air was entrained in water as small sized bubbles. The liquid carried up in the plume splashed and cascaded onto the surface of the bulk liquid. The splashing action in the plume region generated surface waves, which moved towards the side wall opposite to the tuyere.

Because of the asymmetric location of the gas/liquid plume, the major zone of mixing occurred in an area defined by the rising gas/liquid plume and the opposite side of the vessel with respect to the tuyere. The recirculating flows formed by the rising gas/liquid plume generated flows across the surface of the liquid and strong regions of recirculation as depicted in Figure 4. However, a region of relatively stagnant liquid close to the upper corner, opposite the gas injection point persisted.

To model the reduction operation, particles simulating 75FeSi alloy were dropped in the major mixing zone. They were immediately carried away towards the dead zone at the opposite surface corner from the tuyere, where they remained. Apart from the 2 mm diameter particles, larger particles were not easily entrained by the recirculating flow within the main mixing zone, owing to their higher buoyancy forces. The larger particles tended to reduce the chance of smaller particles becoming entrained, by protecting the latter from surface disturbances. With an increase in air flow rates, general flow patterns were hardly affected and particles still had little chance of entrainment.

Slag-covered steel model

In order to simulate typical industrial conditions during the AOD reduction period, the slice model vessel was filled with zinc chloride solution of 500 mm depth to represent liquid steel and covered with silicone oil 50 mm thick to simulate the slag cover. Air was blown into the vessel at various flow rates ranging from 10 to 120 SLPM. To examine the effect of the density of process gas on horizontal penetration and to better respect air/steel density ratios, helium was also injected into the vessel at a flow rate of 226 SLPM. The presence of the silicone oil led to several

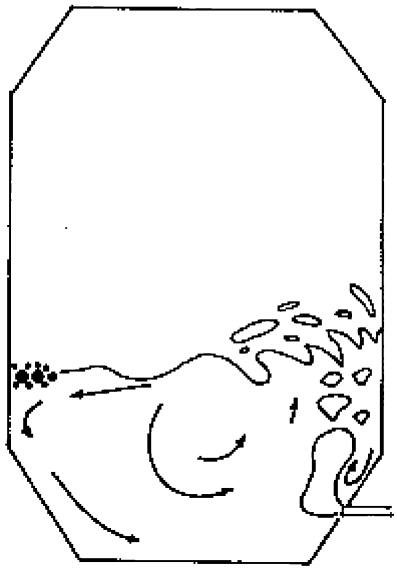

Figure 4. Schematic of induced fluid flows and mixing behaviour of simulated ferro-silicon granules and lumps in the slice 2D model in the absence of a slag phase

significant alterations in the structure of the flow generated within the bulk 'metal' phase and emulsified 'slag/metal' region. Air injection resulted in the generation of many droplets of zinc chloride (steel) and silicone oil (slag) and mixed them thoroughly to form an emulsion. As with the single phase (slag-free steel melt) experiments, the same gas/liquid plume behaviour and asymmetric mixing zones were observed. The horizontal (forward) penetration of the injected air was small and limited to the range of 50 to 150 mm from the tip of the tuyere, depending on the air flow rate. Helium at a flow rate of 226 SLPM led to no increase in the horizontal penetration of the jet plume. While any approximate penetration of only 100 mm was observed in the experiment, the expansion angle using helium was found to be much larger than that for air as gas exited from the tuyere. This resulted in more intense turbulence within the gas/liquid plume vs. air. As with the slag free model, the gas/liquid plume in the present slag-covered steel model was again deflected towards the backwall during its ascent as a result of fluid recirculating back towards the plume from the major mixing zone.

As before, a smaller mixing zone was found between the plume and the tuyere side wall. Because of the high speed of liquid recirculation there, retention times of particles simulating 75FeSi alloy were very short, and any entrained particles in this zone were observed to quickly return to the major mixing zone, as aniticipated. If this smaller mixing zone could be enlarged in commercial AOD vessels, the slower rates of recirculation may have a significant impact on reducing refractory erosion.

As for the case of the single liquid phase experiment, the major mixing zone was situated in the wide area between the plumes and the side wall opposite to the tuyere. This main mixing zone had an emulsified phase on top of the simulated steel melt. The emulsified phase extended beyond the original 'slag/metal' interface, forming an extensive emulsified zone on top of 'steel melt'. The existence of an interface between the emulsified phase and the 'steel melt' resulted in two different recirculating flow patterns: one in the emulsified zone and the other in the 'steel melt'.

Figure 5 depicts the relative positions of the emulsified phase and 'steel melt' and recirculating flow pattern in them. The formation of the emulsion facilitated the entrainment of the particles representing 75FeSi alloys in this zone. The particle were well dispersed by recirculating flows in this region. Smaller particles were entrained more easily and were scattered widely by the recirculating flows. The extent of particle dispersion was constrained to the general area of the impact region of the cascading liquid, as shown in Figure 5. This region of dispersion did not increase significantly with increased air flow alone. However, when the model vessel was tilted 10° clockwise and the airflow increased to 120 SLPM, the extent of the recirculatory flow was significantly enlarged, and entrained particles became more widely dispersed.

Three-dimensional model

Slag-free steel model

Experiments were carried out for the six sets of conditions listed in Table I. Under the experimental conditions for Case 1, the particles added were found to resurface quickly (~0.2 s) and remain on the surface due to their buoyancy.

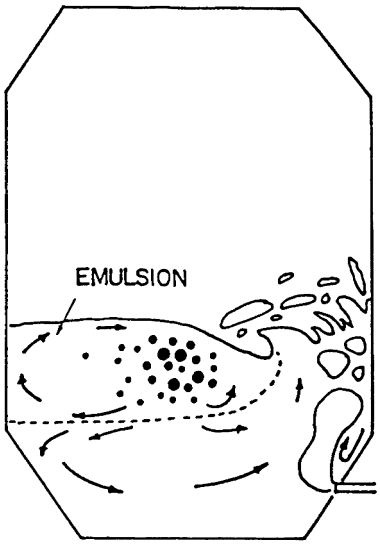

Figure 5. Schematic of induced fluid flows and mixing behaviour of simulated ferro-silicon granules and lumps in the slice 2D model with simulated slag phase

Table I
Experimental conditions for slag covered steel model

Oil/ZnCl(50mm/420mm) Experiments	Flowrate (SLPM)	No. of tuyeres	Particles
Case 1	28.3	5	d_p=14.2mm,ρ_p=800kg/m^3
Case 2	28.3	1	Same as case 1
Case 3	42.5	1	Same as Case 1
Case 4	56.6	5	Same as case 1

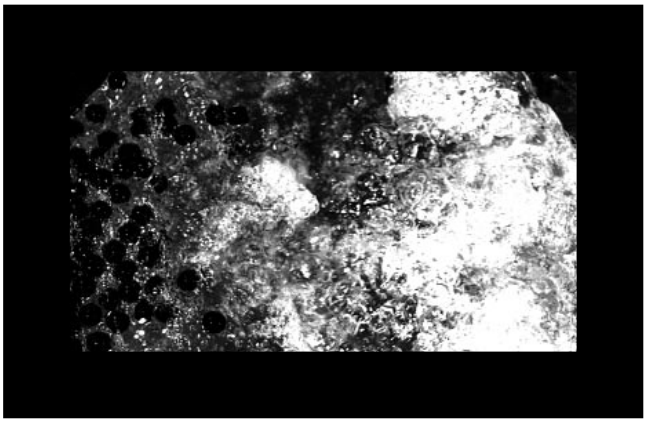

Figure 6. Top view of three-dimensional water modelling experiment; five tuyeres issuing air at 28.3 SLPM generate a rising plume and splashing waves push ferrosilicon alloy additions over to a stagnant zone opposite it

The top view of the flow emanating from the bank of tuyere, as shown in Figure 6, illustrated the waterfall effect that pushes all the particles to the opposite side of the vessel away from the tuyere line. As also noted, splashing generated by the gas-liquid plume above the tuyere was quite considerable and intense. This splashing led to much enfolding of liquid and to gas bubbles.

A side view of the equipment (i.e., adjacent to the tuyeres) showed that the 5 plumes hugged the vertical sidewall in exactly the same fashion as was observed in the slice-model results already reported. Observations during experiments at higher flow rate, e.g. Case 2 and Case 3, indicated the slight increase in penetration of the plume towards the centre, owing to increased momentum of incoming gas. Despite the violent turbulence and enfolding waves, the particles remained floating at the liquid-air interface in the zone opposite the tuyere, apart from occasional subsurface entrainment of a particle. Evidently, from a recovery point of view, such situations should be avoided.

In the experiment for Case 4, similar flow rates (28.3 SLPM) were passed through 1 tuyere rather than 5 tuyeres. The results in terms of particle behaviour were compatible with the results for the five-tuyere experiment, Case 1. However, the penetration of the jet was significantly increased owing to increased momentum of the incoming gas. At increased air flowrates, Case 5 and Case 6, the jet penetrated more than half of the vessel diameter and the plume rose from the other half of the vessel opposite to the tuyeres. Under these circumstances, the spherical particles simulating 75FeSi alloy additions were found to congregate at the same side as the tuyere bank, indicating a shift of 'dead' zone due to the change in flow pattern.

Slag-covered steel metal

In these experiments, a zinc chloride bath with a depth of 420 mm was employed, with a 50 mm thick layer of silicone oil atop. Some wooden spheres of 14.2 mm diameter were used to simulate 75FeSi alloy. These particles were significantly more dense than previous particles, their density being 800 kg/m^3. As such, their specific gravity with respect to zinc chloride is 800/1700, or 0.47, in keeping with the relative density ratio of 0.4 for 75FeSi to steel. Experimental conditions are listed in Table I.

Figure 7. Top view of surface of the 3D model for slag/metal simulation, using zinc chloride-silicone oil

A flowrate of 28.3 SLPM through the five tuyeres was chosen for the first experiment. It was observed that many particles within the emulsified region returned back towards the plume along the sidewalls. These particles where then lifted back into the two-phase region by the plume, only for them to return again. This indicated that the particles were attracted towards the plume and occupied a subsurface region in keeping with their density ratio to the lower zinc chloride phase and the upper oil-zinc chloride emulsion.

A top view of the oil phase (Figure 7) showed that it was transformed into a foam that was very reminiscent of the foaming observed in direct smelter vessels, such as the AISI reactor. One interesting aspect gained from these observations of the top surface of this foam, was that particles were sometimes carried up behind the rising gas bubbles. When bubbles erupted through the surface, one could occasionally see these particles at the base of these bubble eruptions. Summarizing, the particles were well mixed into the 'slag-metal' foam, and no dead zones or accumulations of particles far from the tuyere could be observed. This result was fully in keeping with the results using the thin-slice model.

Equivalent results at 28.3 SLPM using 1 tuyere (Case 2) rather than 5 were observed. Once again, particles were seen recirculating in the immediate vicinity of the rising plume of gas bubbles. As before, they occupied a subsurface region below the foaming slag surface. The violent splashing observed in the single-phase results was somewhat modified in the case of two liquids, and the violence of the intermixing process was not transmitted so significantly to the upper surface. As for the case of five tuyeres, the particles were observed to encircle the vessel and move back towards the column of gas. As such, there were no apparent dead zones in the vessel.

In the last experiment (Case 4), a greater amount of gas (56.6 SLPM) was passed through 5 tuyeres rather than one. This allowed a higher specific energy input to the system to be made without running into difficulties with surface waves. This points to the principle that more gas can be injected into a metallurgical vessel if it is done in a dispersed way, and must clearly be a factor in the design of AOD vessels.

Discussion

Table II gives a summary of numerical values of different modelling criteria for fluid flow in the present study. The specific gas flow rate, *Qm,* is also included for comparison

Table II
Comparison of Modelling Criteria for Flow Behaviour

Criteria	Prototype	Model
F_r'	6.08~24.32	0.91~3.64
ε_m ,W/kg	8.41~23.30	1.39~11.01
Q_m,Nm/s/kg	$6.67x10^{-6}$~13.34x10	$3.77x10^{-6}$~$7.54x10^{-6}$

In the present experiments, higher gas flow rates were impractical owing to the heavier emulsification and foaming of the oil $ZnCl_2$ system than that expected for the slag/metal system. Nevertheless, as seen from Table II, the numerical values of the modified Froude number, specific energy input, and specific gas flow rate have almost the same order of magnitude, suggesting the similarity of fluid flow between the prototype and model vessels.

The present model study shows something in common with respect to the fluid behaviour. Under all experimental conditions, the submerged sideways injection of the processing gas creates two asymmetrical mixing zones, the smaller mixing zone being defined by the plume and the tuyere containing side wall, and the larger main mixing zone situated in the opposite side of the tuyere. It shows that the mixing zone is very limited, and characterized by fast recirculatory flows. The proximity of such an intensively stirred zone to the sidewall can be expected to cause severe refractory erosion above the line of the tuyeres. This is commonly observed in practice.

The problem may presumably be alleviated somewhat by enlarging this mixing zone so as to slow recirculation. One method whereby this can be achieved is by tilting a side-blown vessel so as to bring the rising curtain of plumes more towards the centre of the vessel. The other, larger, main mixing zone, defined by the area confined by the plume and the side wall opposite to the tuyeres, is the region where most 75FeSi alloy particles can be expected to be entrained and participate in the reduction. Therefore, the mixing efficiency of, and its effect on, the dissolution kinetics in the major mixing zone determine the performance of 75FeSi alloy during the reduction period.

Based on the experimental observations, one basic conclusion to the present work is that 75FeSi alloy additions can be easily entrained in the slag phase and have subsurface melting in the AOD operations. Figure 7 gives estimates of the required minimum entrainment velocities for 75FeSi alloy additions to steel and slag baths for various sizes of sphere. One sees that minimum entrainment velocities are significantly smaller than those for Fe-Si in a steel bath. This is mainly due to the small density difference between 75FeSi alloy and slag and to the high viscosity of slag.

Also noted from Figure 7 is the fact that small particles are more readily entrained than larger ones, in agreement with experimental observation. This figure also indicates the difficulty of entraining 75FeSi alloy additions into a steel bath unless small particles are used, and explains the improvement of recovery efficiency when small granular alloy particles vis-à-vis large lumpy alloys were tested in practice. At the high specific gas flow rates used in AOD steelmaking (0.4 Nm^3/min/ton to 0.8 Nm^3/min/ton), considerable amounts of steel are ejected from the vessel. In addition, ferroalloys are normally added into the eye of the rising gas/liquid plume, in order to have fast and wide distribution of alloy particles within the slag bath. As a consequence, a steel or slag shell will first freeze around the Fe-Si alloy additions when they fall into the slag bath. Thus, similar melting behaviour to the work carried out on ferroalloys melting or dissolving in baths of liquid steel, can be expected[6-8].

As such, alloy melting/dissolution times can be estimated by calculating the times required for the convective heat input from the bath to match the total enthalpy requirements needed to raise the additions up to the melting point of steel, i.e.:

$$\rho_p V_p[C_p(T_m - T_0) + \Delta H_m] = h_c A_p \Delta T_{\text{super heat}} \Delta t$$

where ρ_p is density, V_p volume, C_p heat capacity, T_m melting point of steel, T_0 room temperature, ΔH_m heat of melting, h_c heat transfer coeficient, A_p surface area of particle, $\Delta T_{super\ heat}$ degree of super heat of steel, and Δt melting time. This analysis represent a limiting case for

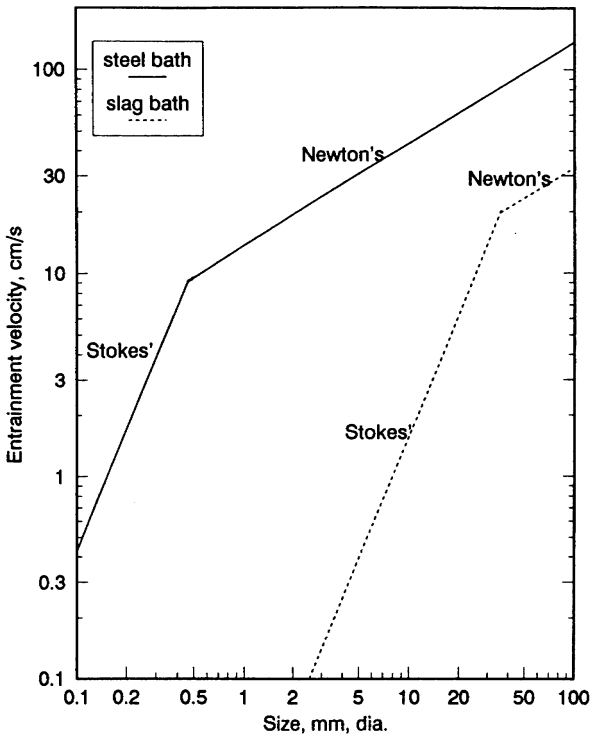

Figure 8. Minimum predicted entrainment velocities for variously sized 75% ferro-silicon alloy additions to become entrained within homogeneously stirred melts of steel and slag

situations in which the Biot number is low (about 0.1) and $T_{m,ferroalloy} < T_{m,steel}$. The above equation shows that for varying ferrosilicon sizes and shapes, other properties and conditions being constant, the melting time, Δt, becomes a linear function of V_p/A_p:

$$\Delta t = K\, V_p/A_p$$

Based on the above Equation, it is readily shown that, for spherical particles, the melting time is linear to particle diameter.

The constant *K* can be obtained from the work by Argyropoulos and Guthrie[7] who showed the melting time of a 25.4 mm diameter of 50FeSi alloy cylinder, immersed in a steel bath of 50°C superheat, taking into account exothermicity, was 35 s. From this information, K = 5.51 s/mm is roughly estimated for 50°C superheat.

It should be noted, depending on the location of alloy addition into the bath, some alloy particles may have a shell of slag/steel emulsion freeze on their surfaces if these particles fall into the emulsified slag/steel phase directly. Under these circumstances, the melting behaviour of ferroalloys is expected to be quite different from the case with a steel shell, as just discussed. First of all, since the melting point of slag (~1200°C[5]) is lower than that of 75FeSi (1300°C[5]), the slag component of the frozen slag/steel shell will remelt prior to the melting of the ferroalloy, with an un-melted steel component remaining on the surface of the ferroalloy. As a result, unlike the case with a frozen steel shell, the ferroalloy will melt and release the molten ferroalloy into the slag directly, once the object reaches the melting temperature of ferroalloy. Secondly, because of the direct contact between the ferroalloy and the slag, the melting process of the ferroalloy will certainly be coupled with the reaction between the ferroalloy and the slag. This coupling effect will result in a very complicated melting behaviour of ferroalloy, which is beyond the scope of the present research work.

Conclusions

Particle intermixing behaviour observed in both the two-dimensional slice model and the fifth scale three-dimensional AOD model for simulating alloy additions led to similar results. The ascending gas/liquid plumes from the tuyeres created two asymmetric mixing zones: a smaller, higher speed, recirculation zone adjacent to the tuyere side wall and a much larger main mixing zone, in the bulk of the reactor. The deoxidation reaction with silicon additions takes place in this larger zone, and the processing efficiency during the reduction period is expected to be governed by the thermal behaviour of the ferroalloys, given their efficient intermixing within the slag-metal emulsion zone. To enhance the kinetics of chromium recovery, small alloy particles are suggested, given their wider distribution, short melting times, and larger interfacial areas provided for slag reduction. Similarly, in order to alleviate the preferential erosion of the refractories above the line of tuyeres due to fast recirculatory flows between the plume and the tuyere containing side wall, results suggest that side-blown vessels be tilted so as to bring the rising curtain of plumes more towards the centre of the vessel.

References

1. LIN, Z. The modeling of emulsification, slag foaming and alloy addition behaviour in intensively stirred metallurgical reactors. Ph.D.Thesis, 1997, McGill University;
2. MAZUMDAR, D. and GUTHRIE, R.I.L. The physical and mathematical modeling of gas-stirred ladle systems, *ISIJ International*, vol. 35 1995, no. 1. pp. 1–20.
3. MAZUMDAR, D., NAKAJIMA, H., and GUTHRIE, R.I.L. Possible roles of upper slag phases on the fluid dynamics of gas stirred ladles, *Metallurgical Transactions*, vol. 19B, June 1988, pp. 507–51.
4. MORI, K. and SANO, N. Process kinetics in Injection Metallurgy, *Tetsu-to-Hagané*, vol. 67, no. 6, 1981. pp. 24–47.
5. GUTHRIE, R.I.L. Engineering in Process Metallurgy, Clarendon Press, Oxford, 1989.
6. GUTHRIE, R.I.L. Alloy addition kinetics in Steelmaking *Electric Arc Furnace Conference Proceedings*, ISS of AIME, Chicago, 35 1977, pp. 30–41.
7. ARGYROPOULOS, S.A. and GUTHRIE, R.I.L. The exothermic dissolution of 50wt% ferro-silicon in molten steel *Canadian Metallurgical Quarterly*, vol. 18, no. 3, 1979, pp. 267–281.